Biotechnology and Bioprocess Engineering 20: 948-955 (2015)
DOI 10.1007/s12257-015-0176-z

RESEARCH PAPER

Characterization of Hydroxyapatite-coated Bacterial Cellulose Scaffold for Bone Tissue Engineering

Sung-Jun Ahn, Young Min Shin, Se Eun Kim, Sung In Jeong, Jin-Oh Jeong, Jong-Seok Park, Hui-Jeong Gwon, Da Eun Seo, Young-Chang Nho, Seong Soo Kang, Chong-Yeal Kim, Jung-Bo Huh, and Youn-Mook Lim

Received: 16 March 2015 / Revised: 25 June 2015 / Accepted: 18 July 2015

Abstract The goal of this study was to develop a novel hydroxyapatite (HA) coated bacterial cellulose (BC) scaffold for bone tissue regeneration. HA-coated BC was prepared by immersing in 30 mL of 5× simulated body fluid at 37°C for 12 h. The resulting HA-coated BC scaffolds were characterized by scanning electron microscopy (SEM), attenuated total reflectance-Fourier transform infrared (ATR-FTIR) spectroscopy, and thermal gravimetric analysis (TGA). HA spherical globules were newly formed on the surface of the BC, and a fibrous network of BC scaffolds still maintained their dimensions for cell adhesion and proliferation. ATR-FTIR spectroscopy analysis showed bands assigned to specific signals for phosphate and carbonate ions from HA. HA-coated BC scaffolds of thermal gravimetric analysis presented residue of around 25%. The ability for bone regeneration of HA-coated BC scaffolds was evaluated using a rat calvarial defect model for 4 and 8 weeks. After implantation, both BC and HA-coated BC scaffolds showed new bone formation derived from existing bone, and found new bone even inside the scaffold. Furthermore, a new bone area was signigicantly increased in the HA-coated BC scaffolds compared with those from BC scaffolds, and bone-like materials were frequently found in HA-coated BC scaffolds. Therefore, the HA-coated BC scaffolds can be used as an effective tool for bone tissue regeneration.

Keywords: bacterial cellulose, radiation, hydroxyapatite, bone tissue engineering

Sung-Jun Ahn†, Young Min Shin†, Sung In Jeong, Jin-Oh Jeong, Jong-Seok Park, Hui-Jeong Gwon, Da Eun Seo, Young-Chang Nho, Youn-Mook Lim*
Research Division for Industry and Environment, Advanced Radiation Technology Institute, Korea Atomic Energy Research Institute, Jeongeup 580-185, Korea
Tel: 82-63-570-3065; Fax: +82-63-570-3079
E-mail: ymlim71@kaeri.re.kr

Se Eun Kim†, Seong Soo Kang
College of Veterinary Medicine, Chonnam National University, Gwangju 61186, Korea

Sung-Jun Ahn, Chong-Yeal Kim
Department of Radiation Science and Technology, Chonbuk National University, Jeonju 561-756, Korea

Jung-Bo Huh*
Department of Prosthodontics, School of Dentistry, Pusan National University, Dental Research Institute, Yangsan 626-870, Korea
Tel: +82-55-360-5144; Fax: +82-55-360-5134
E-mail: neoplasia96@daum.net

†These authors contributed equally to this work.

1. Introduction

Tissue engineering involves the use of biomaterials, and cells can be transplanted with biomaterial-based scaffolds for the regeneration of diseased or damaged tissues. Generally, an ideal tissue engineering scaffold used for tissue regeneration should be biocompatible and biomimetic. For this, biomaterials have been utilized as scaffolds, in which the cells can be seeded, cultured, and then implanted into target tissues to induce or direct the growth of new, healthy tissue. In addition, novel scaffolds have been designed to secrete new substrates such as growth factors to promote cell survival in the body. It can allow favorable cell responses with the surrounding tissue without any inflammatory reaction after being implanted in the body. Therefore, studies on the development and manufacturing of new biomaterials that can be given such properties have been frequently conducted [1].

The scaffolds for hard tissue regeneration can induce efficient tissue regeneration, which should have specific features such as chemical, biological, and mechanical properties [2]. Bone is a hard tissue, which serves to support the structure of the body, and is composed principally of collagen fiber mineralized with hydroxyapatite (HA) mineral crystals (70% of dry weight) and a small amount of a ground substance [3]. HA is a kind of calcium phosphate compound and has consisted in most cortical bone, and cancellous bone except the bone marrow within the bone structure. It has been used as a ceramic biomaterial (bioceramics), because of its excellent biocompatibility and osteoconductive ability [4]. HA primarily used for preparing artificial bone as HA/collagen nanocomposites. However, the utilization of collagen has been limited due to high costs, concerns of cross-infection, and the poor definition of commercial sources [5].

Bacterial cellulose (BC) has been utilized as a scaffold for bone tissue regeneration. In particular, its higher mechanical properties can be suitable for bone tissue regeneration. For instance, BC has a density of 1,600 kg/m^3, a young's modulus of 138 GPa, and a tensile strength of at least 2 GPa, which are almost equal to those of aramid fibers [6]. The BC produced by the *in vitro* synthesis of a polysaccharide of a Gram-negative group of bacteria *Gluconacetobacter xylinus*, has a higher water content, molecular weight, and crystallinity than plant cellulose [7]. The formation of bone-like apatite on the material surface is an essential prerequisite for combination of the artificial materials and bone [8,9]. The bone-like apatite formation can be assessed *in vitro* using a simulated body fluid (SBF) that has almost equal compositions of inorganic ions to human blood plasma [10]. The deposition behaviors of HA from SBF were variously changed in accordance with the concentration of calcium, phosphate, temperature, pH, and the existence of organic or inorganic supplements. Moreover, the deposition behaviors of HA were changed in accordance with the surface characterization of the parent metals [11].

Radiation, such as an electron beam, X-ray, and gamma-ray, has been used to induce the chain scission of the chemical bond or to trigger the chemical reaction within the materials [12,13]. The original properties of the materials are successfully regulated by the radiation exposure. In this study, we used electron beam irradiation to alter the physico-chemical properties of BC scaffolds for promoting HA adsorption. HA coated BC was prepared by Jayasuria's method using SBF for the mineralization of HA on the BC surface. The microstructure, mechanical strength, and thermal properties of the scaffolds were investigated, and we also examined the osteoblast adhesion as well as the new bone formation ability of an HA-coated BC scaffold using the rat calvarial defect model.

2. Materials and Methods

2.1. Chemicals and materials

Hydroxyapatite was purchased from Sigma Aldrich (St. Louis, MO, USA). Bacterial cellulose produced using *Gluconacetobacter hansenii* TL-2C was given from Jadam Co. (Korea) [14], and in this study, the bacterial strain, *Gluconacetobacter hansinii* TL-2C, was incubated for 7 days in a static culture containing 0.3% (w/w) citrus fermented solution and 5% (w/w) sucrose. The pH was adjusted to 4.5 with acetic acid. The obtained gel-like pellicles of BC were purified by immersion in deionized water at 90°C for 2 h and then boiled in a 0.5 M aqueous solution of NaOH for 15 min to remove the bacterial cell remains. The BC was then washed with deionized water several times and soaked in 1% NaOH for 2 days. Finally, the BC pellicles were washed free of alkali. All other reagents and solvents were of analytical grade and used without further purification.

2.2. Preparation of hydroxyapatite-coated bacterial cellulose

BC scaffold (9 cm × 9 cm) prepared by *Gluconacetobacter hansenii* TL-2C was irradiated at 300 kGy with distilled water by an electron beam accelerator (UELV-10-10S, Russia), and then lyophilized. For HA coating, the 5× SBF solution was prepared by Jayasuria's method with the composition of Table 1 [15]. The BC was reacted in 30 mL of 5 × SBF at 37°C for 12 h. Reacted BC was washed with distilled water, and then dried for 48 h at room temperature.

2.3. Scanning electron microscope (SEM) analysis

SEM images of the BC surfaces were obtained on SEM equipment (JSM-6390, JEOL, Japan) operating at 10 kV and at a 10 ~ 12 mm distance. The samples were deposited on a steel plate and coated for 60 sec with gold.

2.4. Attenuated total reflection fourier transform infrared spectroscopy (ATR-FTIR) analysis

Infrared spectra of the BC were recorded using Bruker TEMSOR 37 (Bruker AXS. Inc., Germany) equipped with ATR mode over the range of 500 ~ 4,000/cm at a resolution

Table 1. Amounts of reagents used to create 5× SBF

Reagent	5× SBF (g)
1. NaCl	40.62
2. KCl	1.86
3. $CaCl_2$-$2H_2O$	1.84
4. $MgCl_2$-$6H_2O$	1.52
5. NaH_2PO_4	0.60
6. Na_2SO_4	0.36
7. $NaHCO_3$	1.76

of 4/cm averaged over 32 scans.

2.5. Thermal gravimetric analysis (TGA) and investigation of HA coating stability

A thermo gravimetric analysis was performed using TA Q600 (TA Instrument, USA). Fifteen milligrams (15.0 mg) of the BC prepared was placed in a platinum pan. The analysis was performed at a heating rate 10°C/min from 40 to 800°C under a nitrogen flow. To determine HA coating stability, we immersed the HA-coated BC scaffolds in DW and shake them at 200 rpm for 5 days. Following the incubation, the HA-coated BC was freeze-dried and the surface of the BC was observed using SEM.

2.6. Measurement of mechanical properties

The BC and HA-BC were evaluated for their mechanical properties using a Universal Testing Instrument (Instron 5569, Instron, USA) with a 5 kN load cell and crosshead speed of 10 mm/min. The samples were cut into a 5 mm width × 30 mm length. The tensile strength, tensile strain at break, and young's modulus were determined.

2.7. Immunofluorescence staining

For fluorescent staining, MG63 (4×10^4 cells/scaffold) were seeded on the BC scaffolds. After 1 days of culture, the specimens were fixed using 3.7% paraformaldehyde for 15 min and the cells were then permeabilized in a cytoskeletal buffer solution (0.29 g NaCl, 0.5 mL Triton X-100, 0.06 g $MgCl_2$, 10.30 g sucrose, 0.47 g HEPES buffer, in 100 mL water, pH 7.2) for 10 min at 4°C. After blocking with 1% BSA for 1 h at 37°C, the fixed cells were incubated with 1:200 rhodamine-phalloidin for 1 h at 37°C. The specimens were mounted on glass slides with Vectorshield mounting medium (Vector Laboratory, Peterborough, UK). Immunofluorescence images were obtained using a fluorescent microscope (DMI 4000B, Leica, Wetzlar, Germany). The projected cell spreading area and adherent cell number were analyzed by Image J (NIH, USA).

2.8. Histological analysis

Specimens were fixed with 10% buffered formalin and were decalificated with Calci-Clear^{TM} Rapid (National diagnostics, Atlanta, USA). The samples were then dehydrated in an ascending series of alcohol rinses, and were embedded in a paraplast (Sherwood Medical Industries, St. Louis, USA). The embedded specimens were sectioned to a thickness of 5 μm with a microtome (Reichet-Jung 820). Slides were stained with hematoxylin and eosin (H&E), and were observed under a microscope.

2.9. Statistical analysis

All data are presented as mean ± standard deviation (n = 3). The statistical significance was assessed using a Student's *t*-test ($p < 0.05$).

3. Results and Discussion

3.1. Scanning electron microscope (SEM)

Bacterial celluloses have been known to have a nanofibrous structure [16]. Its diameter, length, and dimension are different according to the bacteria species, general structure resembles with that from native ECM [17]. For instance, Adam M. sokolnicki *et al.* has reported that bacterial

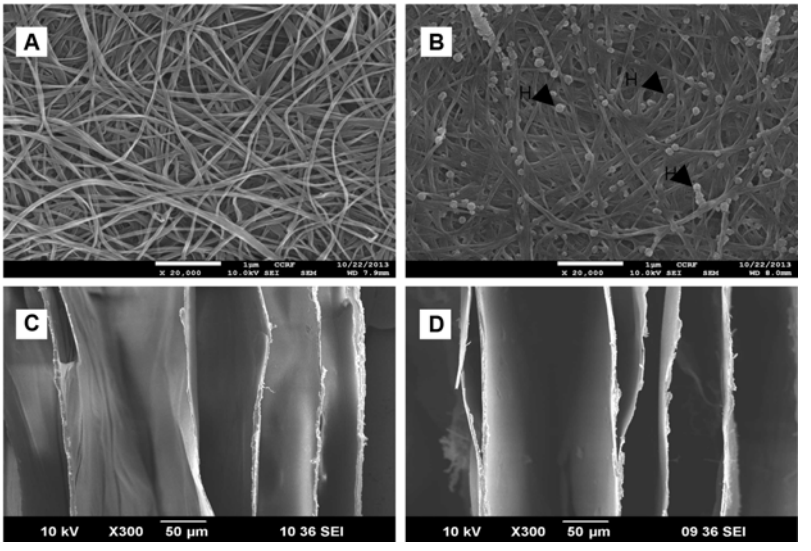

Fig. 1. SEM images of (A) surface of BC and (B) HA-coated BC immersed in 5 × SBF, (C) cross-section views of BC and (D) HA-coated BC immersed in 5 × SBF.

cellulose from membranes exhibited 30 nanometer of fiber diameter; the porosity was 94% [18]. To determine the change of nanofibrous structure of the bacterial cellulose, we observed the morphology of BC before and after HA coating. As shown in Fig. 1, we could not find the morphological differences between BC and HA-coated BC. All BC shows fibrous structures with similar diameters. There was no deformation or breakage after electron beam irradiation. After soaking in SBF, HA spherical globules were newly formed on the surface of BC [19]. At the cross section, the structure of the BC was a physical 3D-network with an upper layer. There was an increasing interval of the layers after irradiation. A dimension of 50 ~ 100 μm between the layers was given as a space where the cells can proliferate inside. Previously, we found that the HA was homogeneously coated on the BC, in which generation of HA spherical globules was regulated by altering immersion time in a SBF solution and concentration [20]. Even though HA-coated BC showed relatively low content of HA globules at the surface, it seems to be resulted by different immersing time in the SBF solution. Therefore, we found that the electron beam-exposed BC allowed strong HA binding.

3.2. Attenuated total reflection fourier transform infrared spectroscopy (ATR-FTIR)

As considering the molecular structure of bacterial cellulose, a hydroxyl group reveals in bacterial cellulose as a representative functional group [21]. It can be the reason why the cellulose can adsorb a higher content of water [22]. Even under electron beam exposure, there was no alteration of BC spectrum in FTIR (data not shown), and we have traced the change of FTIR spectrum after HA coating. Fig. 2 shows typical peaks from BC at 3400/cm (O-H stretching), and 2900/cm (C-H stretching), and HA-coated BC also presented same peaks. However, the peak intensity of O-H stretching and C-H stretching was decreased after immersion in SBF, which might occur by HA adsorption on the surface of BC. Furthermore, we found new signals at 1105, 1028, and 600/cm on the HA-coated BC, which seems to be attributed to the vibrational modes of PO_4^{3-} ions from HA, indicating that it was successfully coated on the surface [23,24]. Consistent with our result, same signals were utilized to determine the presence of HA on BC membrane [25]. Therefore, we concluded that HA was successfully coated at the surface of BC.

3.3. Thermal gravimetric analysis (TGA) and coating stability

Fig. 3A shows the TGA results of BC exposed to an electron beam. A thermal gravimetric analysis was carried out to estimate the thermal stability and degradation properties of the BC and HA-coated BC. The decomposition of the BC and HA-coated BC led to a weight loss at around 320 ~ 350°C. These could have resulted from a cellulose degradation process, including depolymerization, dehydration, and decomposition of glucosyl units followed by the formation of a charred residue. At the HA-coated BC (300 kGy), the initial degradation temperature (T_d) was decreased against the BC (300 kGy) because of phosphorylation on the BC [26]. A carbonaceous residue of around 13% was observed in the BC and 18% in the BC (300 kGy) at 700°C. HA-coated BC (300 kGy) composites presented a residue of around 25%, confirming HA deposition on the BC, which means that the HA content was around 7%. Similar thermal gravimetric analysis was reported by Shengnan Zhang *et al.* After 24 h of SBF solution immersing, HA-coated BC revealed that approximately 50% of residue at 700°C, which resulted by coated HA [27]. Therefore, we found that similar HA coating process allowed HA deposition at the surface.

Next, we investigated HA coating stability at the surface. Previously, the coating stability has been determined by

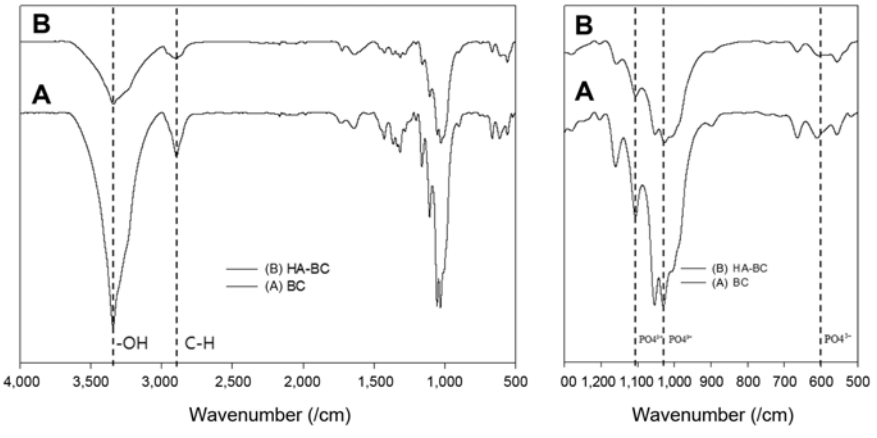

Fig. 2. ATR-FTIR spectra of (A) BC and (B) HA-coated BC immersed in 5 × SBF.

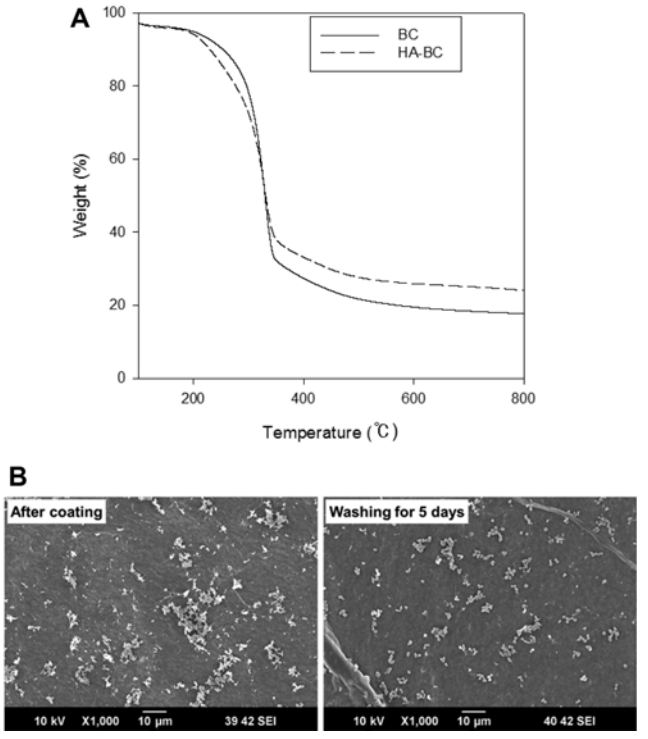

Fig. 3. TGA and HA coating stability (A) TGA curves- solid line for BC, dashed line for HA-coated BC, and (B) SEM images of HA-coated BC before and after vigorous washing for 5 days.

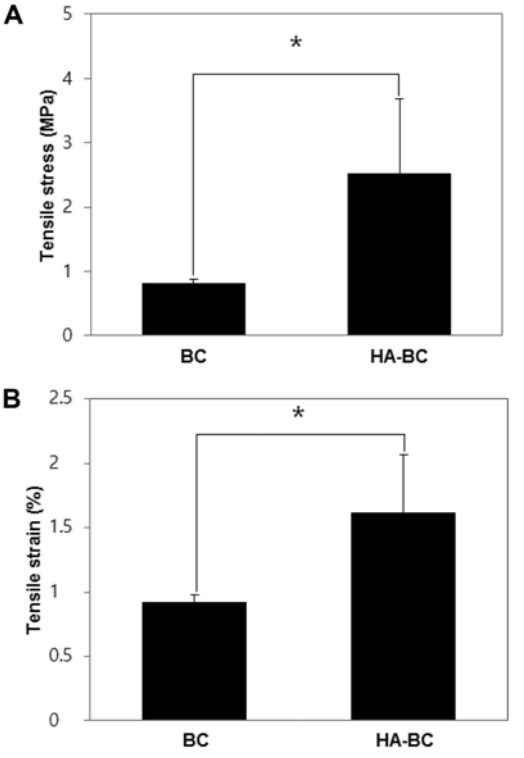

Fig. 4. Mechanical property of BC. (A) Tensile stress and (B) tensile strain. The "*" symbol indicates a significant difference ($p < 0.05$).

vigorous shaking or ultrasonication for predetermined time [28]. As shown in Fig. 3B, HA spherical globules was located at the surface after the coating, in which some of HA looks loosely be bound at the surface. Following the vigorous washing for 5 days, we still found HA globules, loosely attached HA may be detached from the surface. However, most of the HA globules frequently observed at the surface, indicating that the HA was strongly coated at the BC surface.

3.4. Mechanical properties

Bacterial cellulose has been known to have ultimate mechanical property. For example, it has been reported to have 2 GPa of tensile strength [6] and it has been utilized in industry as an additional supplement for enhancing mechanical property such as construction materials, housing for electronics [29]. To examine effect of HA coating to the pristine mechanical property of BC, we measured tensile stress and tensile strain using a universal testing machine. First, we investigated the effect of electron beam irradiation to the pristine property of BC. Electron beam is a strong ionizing source that can be utilized for ion implantation or free radical formation for graft polymerization [30]. In addition, because it can induce chain incision of natural polymer, its usefulness has been increased in degradation control of natural polymer for biomedical applications [31]. In this study, the tensile stress of irradiated BC was drastically decreased to about 6% than that from non-irradiated BC (data not shown), and the deformation and transformation of crystalline with irradiation may cause a decrease in the tensile stress. The mechanical properties of BC before and after HA coating are shown in Fig. 4A. Tensile stress of BC (irradiated) was 0.81 ± 0.06 MPa, which was increased to 2.53 ± 1.15 MPa after immersion in an SBF solution. It might be occurred by deposition of HA globules at the surface. Furthermore, we found that tensile strain was increased after HA coating, it was suggested by synergistic effect of alteration of molecular chain length and HA coating (Fig. 4B). Correctively, HA-coated BC exhibited great mechanical property than the irradiated BC, which might be resulted by homogeneous HA deposition on entire surface as well as inside of the scaffold [32,33].

3.5. *In vitro* cell adhesion and spreading

To determine the effect of coated HA to the cell adhesion and spreading, we seeded MG63 and cultured for 1 day. It is known that HA can improve *in vitro* osteogenic differentiation and *in vivo* new bone formation, and some literatures described enhanced cell viability on the HA

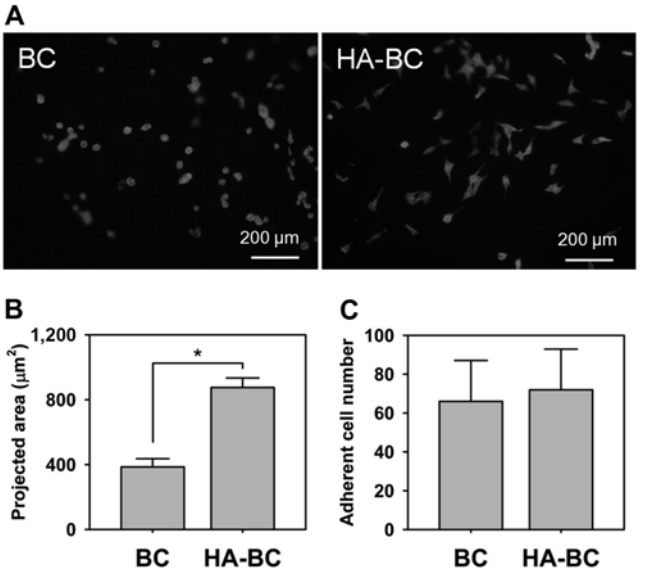

Fig. 5. *In vitro* cell spreading and adhesion. (A) Immunofluorescent staining (red: F-actin), (B) projected cell spreading area (n = 5), and (C) adherent cell number (n = 5). The "*" symbol indicates a significant difference ($p < 0.05$).

coated surface [34]. Adherent MG63 showed spherical shape not to be spread on the BC, it was similar with suspended cell in a solution. However, the adherent cell on the HA-BC exhibited wide spreading morphology (Fig. 5A). The projected cell spreading area on the BC was 385.9 ± 50.3 μm^2, whereas the area on the HA-BC was increased to 875.1 ± 58.7 μm^2 (Fig. 5B). Cell spreading has been regulated by surface property such as hydrophilicity, specific topography, and cell adhesive ligands. In our result, the enhanced cell spreading may be affected by alteration of surface property. In particular, different topography or altered hydrophilicity by coated HA may generate the cell compatible surface, and it looks to regulate the cell spreading. However, we did not find the difference of adherent cell number (Fig. 5C), and its effect looks to be limited in only spreading.

3.6. Histological analysis

At 4 weeks after implantation, in the BC and HA-coated BC groups, the defect regions were filled with fibrous connective tissue within bacterial cellulose as well as spaces between BC (Fig. 6). And both the BC and HA-coated BC groups showed new bone formation derived from the existing bone, and inside the graft. Osteoblast rimming also was observed around the newly formed bone. In particular, active cuboidal osteoblasts were found around the bone-like materials and new bones in the HA-coated BC group, compared that of the B group. Also, in both groups, BC was replaced into the connective tissues and new bone in the defect margin and central region in the

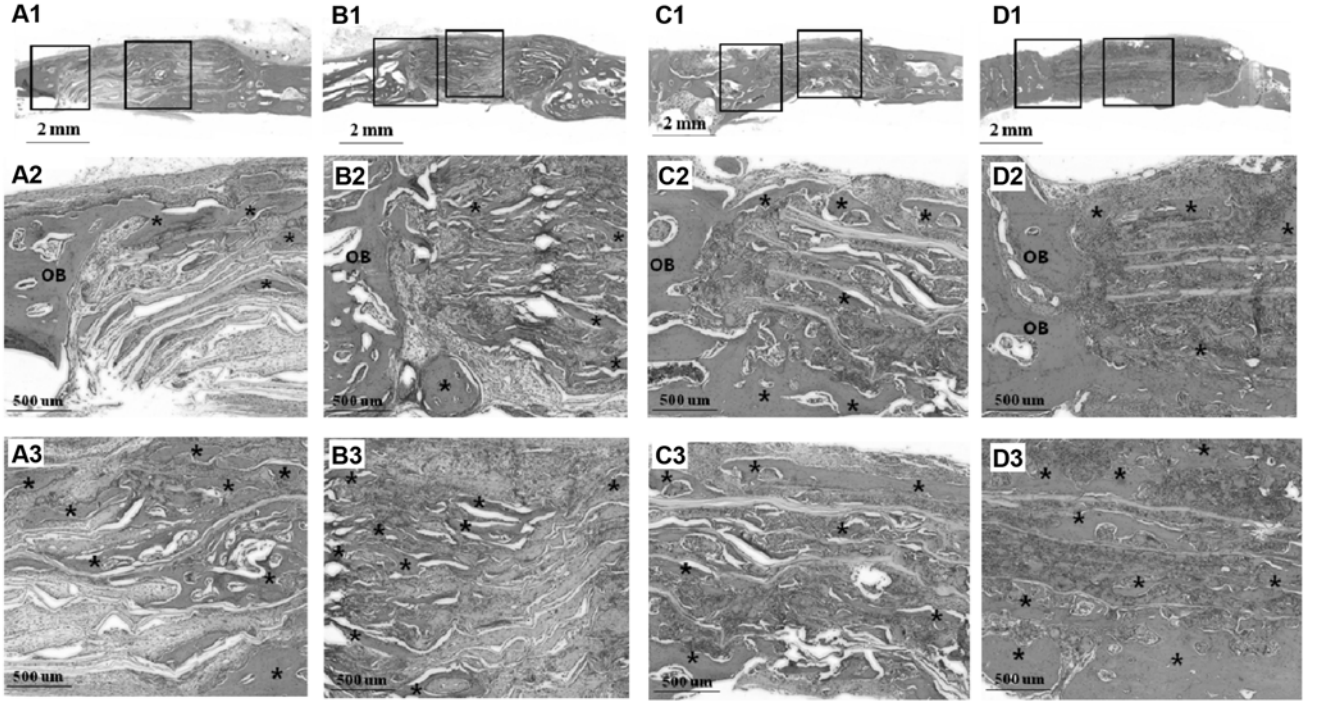

Fig. 6. Histological findings of calvarial defects from rats at 4 and 8 weeks after implantation. (A1-3) BC group at 4 weeks, (B1-3) HA-coated BC group at 4 weeks, (C1-3) BC group at 8 weeks, (D1-3) HA-coated BC group at 8 weeks. Star pattern: newly formed bone, OB: old bone. Specimens were stained with H&E. [A2, B2, C2, and D2; margin of the defect], [A3, B3, C3, and D3; central part of the defect].

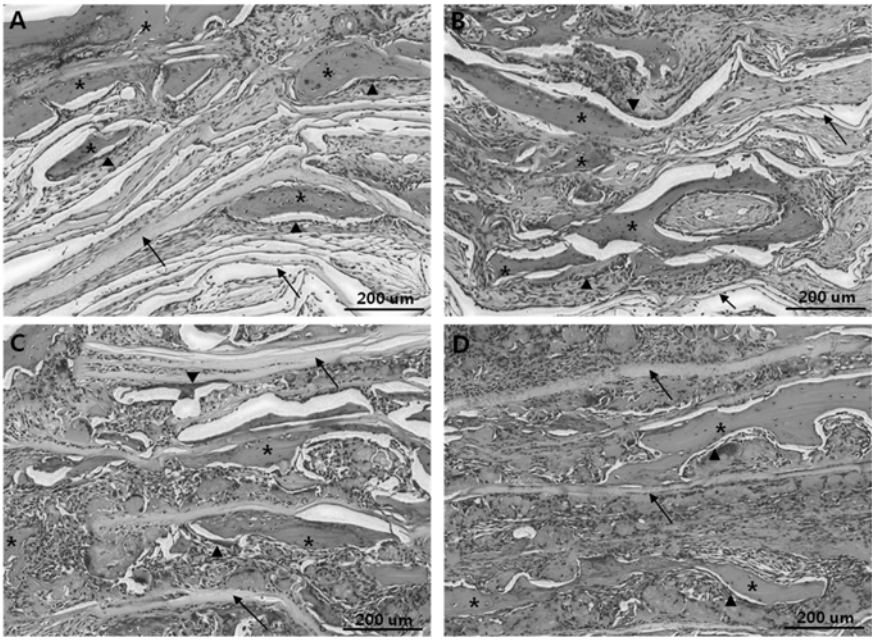

Fig. 7. Histological findings of calvarial defects from rats at 4 and 8 weeks after implantation. (A) BC group at 4 weeks, (B) HA-coated BC group at 4 weeks, (C) BC group at 8 weeks, (D) HA-coated BC group at 8 weeks. Star pattern: newly formed bone, Arrow: bacterial cellulose, Arrow head: osteoblast rimming. Specimens were stained with H&E.

HA-coated BC group, compared to that of the BC group. At 8 weeks, there was more new bone formation within the defect margins and inside the graft than at 4 weeks for all groups. Furthermore, large amounts of bone-like material were found around the remaining cellulose fiber, and more BC was replaced into trabecular new bones. In the HA-coated BC group, more new bone formation and bone-like materials were found, compared to those of the BC group (Fig. 7). In addition, the surrounding field was characterized by a great quantity of osteoblast, fibroblast-like cells. There were no inflammatory reactions observed for any group.

4. Conclusion

HA-coated BC scaffolds were successfully fabricated through the mineralization of BC fibers. Bone regeneration requires a significant mineral component that gives the physiological properties, including its mechanical strength. The results presented in this work confirmed that the inclusion of particles of HA into the irradiated BC surface improves the mechanical properties and incorporates the nanotopographic features that mimetic the structure of natural bone. Moreover, in a histological analysis of HA-coated BC, scaffolds were more effective for bone regeneration than the other samples. The results of this study can be of significance in the fields of biomaterials for bone tissue engineering.

Acknowledgments

This study was supported by National Nuclear R&D program through the National Research Foundation of Korea (NRF) funded by the Ministry of Science, ICT and Future Planning, Korea (2012M2A2A6013196), a grant from Technology Commercialization Support Program, Ministry of Agriculture, Food and Rural Affairs, Republic of Korea (113043-3).

References

1. Langer, R. and D. A. Tirrell (2004) Designing materials for biology and medicine. *Nature* 428: 487-492.
2. Lim, J. Y., S. H. Kim, and Y. H. Kim (2002) Polymeric materials for hard tissue fixation. *Polym. Sci. Technol.* 13: 15-22.
3. Profio, A. E. (1993) *Biomedical Engineering*. John Wiley & Sons Inc, NY, USA.
4. Kawai, N., S. Niwa, M. Sato, Y. Sato, Y. Suwa, and I. Ichihara (1997) Bone formation by cells from femurs cultured among three-dimensionally arranged hydroxyapatite granules. *J. Biomed. Mater. Res.* 37: 1-8.
5. Kong, X. D., F. Z. Cui, X. M. Wang, M. Zhang, and W. Zhang (2004) Silk fibroin regulated mineralization of hydroxyapatite nanocrystals. *J. Cryst. Growth*. 270: 197-202.
6. Hutmacher, D. W. (2000) Scaffolds in tissue engineering bone and cartilage. *Biomater.* 21: 2529-2543.
7. Millon, L. E. and W. K. Wan (2006) The polyvinyl alcohol-bacterial cellulose system as a new nanocomposite for biomedical applications. *J. Biomed. Mater. Res. B: Appl. Biomater*. 79: 245-253.

8. Kokubo, T. (1991) Bioactive glass ceramics: Properties and applications. *Biomater.* 12: 155-163.
9. Hench, L. L. (1991) Bioceramics: From concept to clinic. *J. Am. Ceram. Soc.* 74: 1487-1510.
10. Helebrant, A., L. Jonasova, and L. Sanda (2002) The influence of simulated body fluid composition on carbonated hydroxyapatite formation. *Ceramics*. 46: 9-14.
11. Kim, I. -Y., S. -J. Seo, H. -S. Moon, M. -K. Yoo, I. -Y. Park, B. -C. Kim, and C. -S. Cho (2008) Chitosan and its derivatives for tissue engineering applications. *Biotechnol. Adv.* 26: 1-21.
12. Charlesby, A. (1955) The degradation of cellulose by ionizing radiation. *J. Polym. Sci.* 15: 263-270.
13. Kudoh, H., N. Kasai, T. Sasuga, and T. Seguchi (1996) Low temperature gamma-ray irradiation effects on polymer materials-2. Irradiation at liquid helium temperature. *Radiat. Phy. Chem.* 48: 89-93.
14. Choi, J., S. I. Jeong, and Y. M. Lim (2012) Preparation and characterization of Gelatin-immobilized bacterial cellulose scaffold for tissue engineering using Gamma-ray irradiation. *J. Radiat. Ind.* 6: 159-164.
15. Jayasuriya, A. C., C. Shah, N. A. Ebraheim, and A. H. Jayatissa (2008) Acceleration of biomimetic mineralization to apply in bone regeneration. *Biomed. Mater.* 3: 015003.
16. Backdahl, H., G. Helenius, A. Bodin, U. Nannmark, B. R. Johansson, B. Risberg, and P. Gatenholm (2006) Mechanical properties of bacterial cellulose and interactions with smooth muscle cells. *Biomat.* 27: 2141-2149.
17. Retegi, A., N. Gabilondo, C. Pena, R. Zuluaga, C. Castro, P. Ganan, K. de la Caba, and I. Mondragon (2010) Bacterial cellulose films with controlled microstructure mechanical property relationships. *Cellulose* 17: 661-669.
18. Sokolnicki, A. M., R. J. Fisher, T. P. Harrah, and D. L. Kaplan (2006) Permeability of bacterial cellulose membranes. *J. Membr. Sci.* 272: 15-27.
19. Nge, T. T. and J. Sugiyama (2007) Surface functional group dependent apatite formation on bacterial cellulose microfibrils network in a simulated body fluid. *J. Biomed. Mater. Res. Part A*. 81: 124-134.
20. Wan, Y. Z., Y. Huang, C. D. Yuan, S. Raman, Y. Zhu, H. J. Jiang, F. He, and C. Gao (2007) Biomimetic synthesis of hydroxyapatite/bacterial cellulose nanocomposites for biomedical applications. *Mater. Sci. Eng. C* 27: 855-864.
21. Esa, F., S. M. Tasirin, and N. A. Rahman (2014) Overview of bacterial cellulose production and application. *Agric. Agric. Sci. Proc* 2: 113-119.
22. Martins, I. M. G., S. P. Magina, L. Oliveira, C. S. R. Freire, A. J. D. Silvestre, C. P. Neto, and A. Gandini (2009) New biocomposites based on thermoplastic starch and bacterial cellulose. *Comp. Sci. Technol.* 69: 2163-2168.
23. Figueiredo, M. M., J. A. F. Gamelas, and A. G. Martins (2012) *Infrared Spectroscopy-Life and Biomedical Sciences.* Chap. 11. InTech, 51000 Rijeka, Croatia.
24. Figueiredo, A. G. P. R., A. Alonso-Varona, S. Fernandes, T. Palomares, E. Rubio-Azpeitia, A. Barros-Timmons, A. J. D. Silvestre, C. Pascoal Neto, and C. S. R. Freire (2013) Biocompatible bacterial Cellulose-poly (2-hydroxyethyl methacrylate) nanocomposite films. *Biomed. Res. Int.* 2013: ID 698141.
25. Saska, S., H. S. Barud, A. M. M. Gaspar, R. Marchetto, S. J. L. Ribeiro, and Y. Messaddeq (2011) Bacterial Cellulose-hydroxyapatite nanocomposites for bone regeneration. *Int. J. Biomater.* 8: 175362.
26. Wanrosli, W. D., R. Rohaizu, and A. Ghazali (2011) Synthesis and characterization of cellulose phosphate from oil palm empty fruit bunches microcrystalline cellulose. *Carbohydr. Polym.* 84: 262-267.
27. Zhang, S., G. Xiong, F. He, Y. Huang, Y. Wang, and Y. Wan (2009) Characterisation of hydroxyapatite/bacterial cellulose nanocomposite. *Polym. Polym. Compos.* 17: 353-358.
28. Ryu, J., S. H. Ku, H. Lee, and C. B. Park (2010) Mussel-inspired polydopamine coating as a universal route to hydroxyapatite crystallization. *Adv. Func. Mater.* 20: 2132-2139.
29. Gindl, W. and J. Keckes (2004) Tensile properties of cellulose acetate butyrate composites reinforced with bacterial cellulose. *Compos. Sci. Technol.* 64: 2407-2413.
30. Crivello, J. V. (1999) UV and electron beam-induced cationic polymerization. *Nucl. Instr. Meth. Phys. Res. B* 151: 8-21.
31. Hausberger, A. G., R. A. Kenley, and P. P. DeLuca (1995) Gamma irradiation effects on molecular weight and *in vitro* degradation of poly(D,L-Lactide-co-Glycolide) microparticles. *Pharm. Res.* 12: 851-856.
32. Driscoll, M., A. Stipanovic, W. Winter, K. Cheng, M. Manning, J. Spiese, R. A. Galloway, and M. R. Cleland (2009) Electron beam irradiation of cellulose. *Radiat. Phy. Chem.* 78: 539-542.
33. Scaglione, S., C. Ilengo, M. Fato, and R. Quarto (2009) Hydroxyapatite-coated polycaprolacton wide mesh as a model of open structure for bone regeneration. *Tissue Eng. Part A* 15: 155-163.
34. Kilpadi, K. L., P. -L. Chang, and S. L. Bellis (2001) Hydroxylapatite binds more serum proteins, purified integrins, and osteoblast precursor cells than titanium or steel. *J. Biomed. Mater. Res.* 57: 258-267.